

Claimed detection of PH₃ in the clouds of Venus is consistent with mesospheric SO₂

ANDREW P. LINCOWSKI,^{1,2} VICTORIA S. MEADOWS,^{1,2} DAVID CRISP,^{2,3} ALEX B. AKINS,⁴ EDWARD W. SCHWIETERMAN,^{2,5,6}
GIADA N. ARNEY,^{2,7} MICHAEL L. WONG,^{1,2} PAUL G. STEFFES,⁸ M. NIKI PARENTEAU,^{2,9} AND SHAWN DOMAGAL-GOLDMAN^{2,7}

¹*Department of Astronomy and Astrobiology Program, University of Washington, Box 351580, Seattle, Washington 98195, USA*

²*NASA Nexus for Exoplanet System Science, Virtual Planetary Laboratory Team, Box 351580, University of Washington, Seattle, Washington 98195, USA*

³*Jet Propulsion Laboratory, California Institute of Technology, Earth and Space Sciences Division, Pasadena, California 91011, USA*

⁴*Jet Propulsion Laboratory, California Institute of Technology, Instruments Division, Pasadena, California 91011, USA*

⁵*Department of Earth and Planetary Sciences, University of California, Riverside, CA 92521 USA*

⁶*Blue Marble Space Institute of Science, Seattle, WA, USA*

⁷*NASA/Goddard Space Flight Center, Greenbelt, MD 20771, USA*

⁸*School of Electrical and Computer Engineering, Georgia Institute of Technology, Atlanta, GA 30332-0250, USA*

⁹*MS 239-4, Space Science Division, NASA Ames Research Center, Moffett Field, CA, USA*

(Received October 21, 2020; Revised January 18, 2021; Accepted January 21, 2021)

Submitted to ApJL

ABSTRACT

The observation of a 266.94 GHz feature in the Venus spectrum has been attributed to PH₃ in the Venus clouds, suggesting unexpected geological, chemical or even biological processes. Since both PH₃ and SO₂ are spectrally active near 266.94 GHz, the contribution to this line from SO₂ must be determined before it can be attributed, in whole or part, to PH₃. An undetected SO₂ reference line, interpreted as an unexpectedly low SO₂ abundance, suggested that the 266.94 GHz feature could be attributed primarily to PH₃. However, the low SO₂ and the inference that PH₃ was in the cloud deck posed an apparent contradiction. Here we use a radiative transfer model to analyze the PH₃ discovery, and explore the detectability of different vertical distributions of PH₃ and SO₂. We find that the 266.94 GHz line does not originate in the clouds, but above 80 km in the Venus mesosphere. This level of line formation is inconsistent with chemical modeling that assumes generation of PH₃ in the Venus clouds. Given the extremely short chemical lifetime of PH₃ in the Venus mesosphere, an implausibly high source flux would be needed to maintain the observed value of 20±10 ppb. We find that typical Venus SO₂ vertical distributions and abundances fit the JCMT 266.94 GHz feature, and the resulting SO₂ reference line at 267.54 GHz would have remained undetectable in the ALMA data due to line dilution. We conclude that nominal mesospheric SO₂ is a more plausible explanation for the JCMT and ALMA data than PH₃.

1. INTRODUCTION

Greaves et al. (2020a) recently attributed a 266.94 GHz (1.123 mm) line observed in the Venus spectrum to ~20 ppb of phosphine (PH₃) absorbing above 56 km altitude, in the upper clouds. In the strongly-oxidizing Venus atmosphere, PH₃ formation is disfavored and its destruction is enhanced, leading Greaves et al. (2020a) to argue that its presence in the clouds points to unknown geological, chemical or even biological processes. The discovery team identified no viable abiotic production mechanism for PH₃ in the Venus at-

mosphere (Greaves et al. 2020a; Bains et al. 2020), and so a biological origin was considered. PH₃ has been proposed as a potential biosignature in terrestrial planet atmospheres (Sousa-Silva et al. 2020) due to its association with decaying organic matter (Glindemann et al. 2005), and significant—presumed biological—fluxes from marine environments on Earth (Zhu et al. 2007). However, the specific mode of biological production of PH₃ remains uncertain and is still vigorously debated (Roels & Verstraete 2001), with no known direct metabolic pathway (Roels et al. 2005).

The identification of PH₃ in the Venus clouds was made using multiple observations of a single spectral feature at 266.94 GHz, where both PH₃ (266.944 GHz) and SO₂ (266.943 GHz) have absorption lines (Greaves et al. 2020a). After the initial detection using coadded spectra from the

James Clark Maxwell Telescope (JCMT), which were taken over 5 nights between 2017 June 9–16, follow-up observations were made with the Atacama Large Millimeter Array (ALMA) on 2019 March 5. The latter dataset included simultaneous narrow-band (0.1171875 GHz) and wide-band (1.875 GHz) observations, centered on the Venus rest-frame PH₃ frequency. The 266.94 GHz line, seen in the JCMT data at a S/N of 4.3 (Greaves et al. 2020a; although this detection significance has been subsequently called into question, Thompson 2020), was also detected in the ALMA narrow-band and wideband datasets at higher significance than in the JCMT data (Greaves et al. 2020a), although a subsequent re-analysis of the ALMA data also suggests a less significant detection, with a correspondingly lower inferred abundance of PH₃ (Greaves et al. 2020b). Assuming a uniform mixing ratio for the PH₃, Greaves et al. (2020a) derive an abundance of 20 ppb from the JCMT observations, and calculate an emission weighting function peaked at 56 km. They therefore conclude that the PH₃ absorption feature was sourced primarily from within the Venus clouds. However, as Greaves et al. (2020a) point out, with a FWHM of 4–5 km s⁻¹, this line could potentially contain contributions from both PH₃ and SO₂, as the SO₂ line center is only +1.3 km s⁻¹ from the PH₃ line center.

Consequently, the PH₃ line identification is strongly dependent on accurately estimating and excluding a potentially-significant contribution from SO₂, which, after the bulk atmospheric gases CO₂ and N₂, is the third most abundant gas in the Venus atmosphere. Greaves et al. (2020a) attempted to quantify the SO₂ contribution to the observed 266.94 GHz feature by searching the ALMA wide-band observations for the nearby, stronger SO₂ $J_{K_a, K_c} = 13_{3,11} \leftarrow 13_{2,12}$ 267.537 GHz line, but did not detect it (see their Figure 4a). Instead, they estimated a 10 ppb upper limit for SO₂, based on potentially large spectral “ripples”, artifacts in the data induced by interferometric response to Venus as a bright, extended source. Greaves et al. (2020a) also noted that the ≤ 10 ppb value was comparable to a 346.652 GHz ALMA Venus SO₂ measurement of 16.5 ± 4.6 ppb, which was taken in 2011 (Piccialli et al. 2017). However, the Piccialli et al. (2017) observation was sensitive to SO₂ at 85 km altitude (Piccialli et al. 2017) in the Venus mesosphere (which extends from 65–120 km), and not to the middle/upper cloud deck (53–61 km). The ≤ 10 ppb constraint derived from the non-detection implied a maximum 10% contribution from SO₂ to the 266.94 GHz absorption band depth, and a shift in the observed line centroid of no more than 0.1 km s⁻¹. Greaves et al. (2020a) concluded that SO₂ had been ruled out as a significant contaminant for the putative PH₃ line. Conversely, they argued that the 266.94 GHz line could not be explained solely by SO₂, because the corresponding reference lines would be significantly stronger than the -0.0006 l:c

(line-to-continuum) ratio limit set by the spectral ripples, and yet the reference lines were not detected.

Because the non-detection of SO₂ by Greaves et al. (2020a) supports a corresponding low inferred abundance, and a low contamination fraction for the 266.94 GHz line, it is the key piece of evidence supporting the PH₃ line identification at 266.94 GHz— and so it warrants closer scrutiny. There is an apparent contradiction between the inferred altitudes that the PH₃ feature probed, and the SO₂ abundance constraint. If the putative PH₃ (266.94 GHz) absorption is sensitive to altitudes near 56 km, and thus probes the Venus middle and upper cloud, then the 267.94 GHz SO₂ reference line should also originate from this altitude range, since it has similar line strength and amount of underlying continuum absorption. Data and modeling estimates place the SO₂ abundance near 1–5 ppm at 60 km in the upper cloud, which should increase with depth to match the higher ~ 130 ppm measured below the cloud deck (Zasova et al. 1993; Krasnopolsky 2012; Zhang et al. 2012; Belyaev et al. 2012; Marcq et al. 2008; Arney et al. 2014; Encrenaz et al. 2019). Previous measurements therefore suggest that the inferred disk-averaged < 10 ppb of SO₂ is anomalously low, especially if the observations probe within the clouds. Assuming similar spatial distribution of the two gases, for an inferred SO₂ abundance at 56 km of 10ppm, and the 10 ppb PH₃ abundance of Greaves et al. (2020a), the SO₂ contribution to the observed line would exceed that from PH₃ by two orders of magnitude (Krasnopolsky 2020).

If the observations were instead sensitive to the mesospheric levels above the clouds, as is the case for higher frequency ALMA observations (Sandor et al. 2010; Encrenaz et al. 2015), then the inferred Venus SO₂ abundance would be closer to, but still lower than previously measured levels (Sandor et al. 2010; Encrenaz et al. 2015; Piccialli et al. 2017; Vandaele et al. 2017). While the abundance of SO₂ above the clouds is known to vary significantly over time (Esposito et al. 1988; Encrenaz et al. 2012, 2019) with a minimum observed around 10–100 ppb at ~ 80 km, the abundances in the mesosphere have been measured to be in the range 10 ppb to 10 ppm (Krasnopolsky 2010; Belyaev et al. 2012; Vandaele et al. 2017). A planet-wide decrease from a higher cloud-top SO₂ abundance in 2006 to a low in 2014 of 30 ppb was also observed, but more recent observations from 2016 through September 2018, which span the Greaves et al. (2020a) JCMT observation, show a strong increase to typical cloud-top values of several hundred ppb of SO₂ (Encrenaz et al. 2019).

While line absorption occurring predominantly within the mesosphere would make the non-detection and inferred low abundance of SO₂ more plausible, it would also suggest that the line attributed to PH₃ was formed at mesospheric levels. Consequently, the 266.94 GHz line would not be sensitive to,

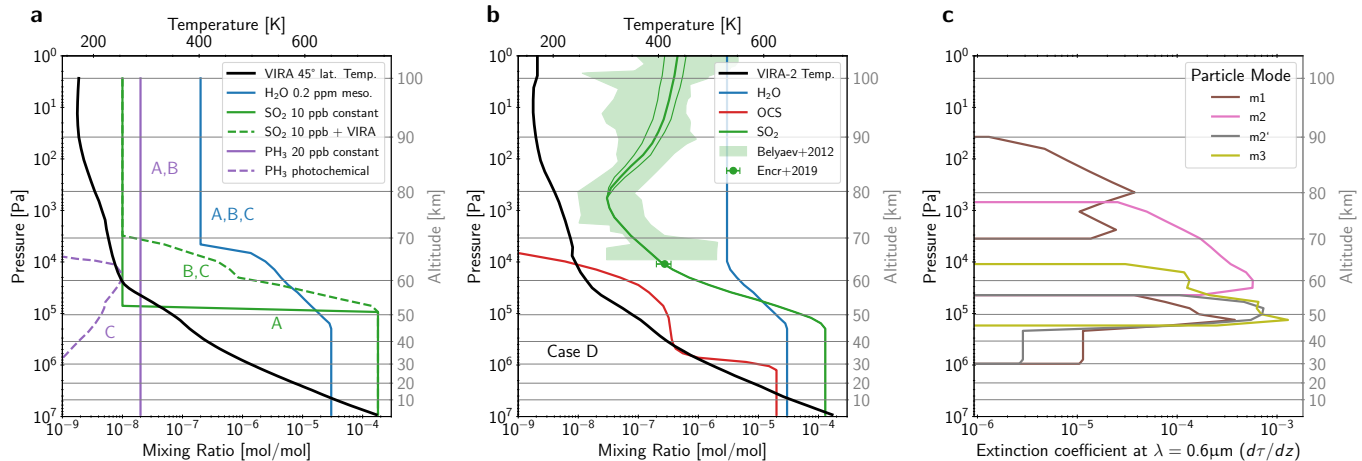


Figure 1. Atmospheric structures for Venus used in our spectral modeling cases. *Panel a:* Temperature and vertical profiles for Cases A–C, which use parameters assumed/derived by Greaves et al. (2020a). Temperature profile (black line) is for VIRA 45° latitude (Seiff et al. 1985), and vertical profiles are shown for PH₃ (solid, Cases A, B; dashed Case C), SO₂ (green), and H₂O (blue). *Panel b:* Temperature and vertical profiles for our Case D best fit to the JCMT 266.94 GHz line. The temperature profile (black line) is from VIRA-2 (Moroz & Zasova 1997). The nominal gas mixing ratios for H₂O (blue line) is based on VIRA values (von Zahn & Moroz 1985) updated for the lower atmosphere (De Bergh et al. 2006) but have also been modified slightly as described in § 2. For OCS (red line), the profile is constructed based on recent measurements by Krasnopolsky (2010) and Arney et al. (2014), and by the surface abundance in the lower atmosphere model by Krasnopolsky (2013). For SO₂ (green line), we fit the 266.94 GHz line guided by the vertical profile of Belyaev et al. (2012) in the mesosphere and upper cloud, and consistent with a suite of SOIR and SPICAV UV SO₂ measurements taken from 2007–2008 (green shaded region). This profile passes through the cloud-top SO₂ measurement (200–350 ppb) obtained by Encrenaz et al. (2019) in July 2017 (green data point), one month after the Greaves et al. (2020a) JCMT observations. We use 130 ppm in the lower atmosphere (Marcq et al. 2008) and generated a profile between the lower atmosphere and cloud tops. *Panel c:* optical depth extinction profiles (optical depth per meter at a wavelength of 0.6 μm) for the Venus cloud particle modes: m1 (haze), m2, m2', and m3 (Crisp 1986). The clouds are defined via optical depth considerations to span approximately 48–70 km (3×10^3 – 1.3×10^5 Pa).

and so not able to confirm, the presence of PH₃ in the Venus clouds—potentially weakening support for a biological origin. The presence of 20 ppb of mesospheric PH₃ would require an extremely large source flux due to photolysis and reactions with radical species, including Cl and H, that result in a sub-second lifetime for PH₃ in the Venus mesosphere (Bains et al. 2020, their Fig. 2). Indeed, the vertical distribution predicted using photochemical-kinetics studies with a cloud source of PH₃ indicates a sharply reduced mesospheric abundance of PH₃ (< 0.001 ppb) alongside significant (> 100 ppb below 95 km) SO₂ (Greaves et al. 2020a, extended data figure 9; Bains et al. 2020).

To explore the potential contradictions posed by the Greaves et al. (2020a) PH₃ observations, and to verify the source region for the 266.94 GHz absorption, here we use a radiative transfer model of the Venus atmosphere to simulate the impact on the Venus millimeter-wavelength spectrum of different abundances and vertical distributions of PH₃ and SO₂, including those proposed by Greaves et al. (2020a) and Bains et al. (2020).

2. METHODS

To generate synthetic millimeter-wavelength spectra of Venus, we use SMART (Spectral Mapping Atmospheric Radiative Transfer), a 1D line-by-line, multi-stream, fully

multiple-scattering radiative transfer model (Meadows & Crisp 1996; Crisp 1997). SMART has been validated against observations of Solar System planets, with heritage modeling the Venus atmosphere (Meadows & Crisp 1996; Arney et al. 2014; Robinson & Crisp 2018).

Our spectral simulations consist of Cases A–C, for which we generate spectra based on the mixing ratios and vertical profiles used and derived by Greaves et al. (2020a), and our best fit model, Case D, which does not contain PH₃ and uses constraints from additional Venus observations (Figure 1). Cases A–C include CO₂, SO₂, H₂O, and PH₃ and use the VIRA 45° latitude temperature profile (Seiff et al. 1985). To match the H₂O estimate of Greaves et al. (2020a), we use the De Bergh et al. (2006) H₂O profile but reduced to 0.2 ppm above 68 km. For SO₂, we use the De Bergh et al. (2006) compilation below 100 km for cases B and C, but reduced to 10 ppb above 70 km, and for case A we maintain 10 ppb down through the cloud deck to 53 km. For PH₃, we use a uniformly mixed 20 ppb profile for cases A and B, and the photochemical profile from Greaves et al. (2020a) (their figure ED7) for case C.

For our best-fit scenario, Case D, we do not include PH₃ and use the De Bergh et al. (2006) update to the VIRA below 100 km and more recent observations where available. We use the VIRA-2 temperature profile (Moroz & Zasova 1997).

For H₂O, we use 30 ppm below the cloud deck (De Bergh et al. 2006, and references therein), and we assume 3 ppm above the cloud deck (Krasnopolsky et al. 2013; Cottini et al. 2015; Piccialli et al. 2017). For SO₂, we use 130 ppm below the cloud deck (Gelman et al. 1979; Bezard et al. 1993; De Bergh et al. 2006; Marcq et al. 2008; Arney et al. 2014), decreasing with increasing altitude to the July 2017 observation of ~ 275 ppb at 64 km (Encrenaz et al. 2019), which was measured within a month of the Greaves et al. (2020a) JCMT data. In the mesosphere, we fit the SO₂ profile to the observed feature at 266.94 GHz guided by the vertical profile fit to 2007–2008 data from Belyaev et al. (2012), which is consistent with the cloud-top SO₂ abundance observed in July, 2017 (see Encrenaz et al. 2019). Long-term monitoring has shown that 2007–2008 and 2017–2018 were similar maximum periods of global mesospheric SO₂ abundance (Encrenaz et al. 2019), although short-term temporal variability within these secular changes can be orders of magnitude (Belyaev et al. 2017). We prescribe the OCS profile guided by recent measurements (Krasnopolsky 2010; Arney et al. 2014) and models (Zhang et al. 2012; Krasnopolsky 2012, 2013; Lincowski et al. 2018). We adopt the same aerosol properties, modes, and optical depth profiles as Arney et al. (2014), which originate from Crisp (1986). Temperature and gas profiles, and aerosol optical depths, are shown in Figure 1.

Absorption cross-sections associated with vibrational-rotational transitions are calculated using a line-by-line model, LBLABC (see Meadows & Crisp 1996; Crisp 1997, for details), with the HITRAN2016 line database (Gordon et al. 2017) for all gases except CO₂, which is calculated from the extensive Ames line database (Huang et al. 2017). Because these line lists assume terrestrial isotopic abundance, we use the methods described in Lincowski et al. (2019) to adjust the line list isotopologue abundances for H₂O to 200 times the D/H abundance compared to Earth, the standard value used in the literature for the Venus mesosphere (Encrenaz et al. 2015). Collision-induced absorption data is used for CO₂-CO₂ (Gruszka & Borysow 1997).

Data on the foreign broadening of gases by CO₂ is not well-characterized, compared to broadening by air, but is more appropriate for Venus simulations. To reproduce the results of Greaves et al. (2020a), we use their foreign broadening parameter for PH₃ of $0.186 \text{ cm}^{-1} \text{ atm}^{-1}$, which they used to estimate PH₃ as 20 ± 10 ppb in the JCMT data. Because their broadening treatment for gases other than PH₃ is not specified, we use the default HITRAN air broadening for cases A–C. To fit the 266.94 GHz detection feature with SO₂ in case D, we employ data for broadening by CO₂, as available. For SO₂ and OCS, we use data for broadening by CO₂ available in HITRAN (Wilzewski et al. 2016; Gordon et al. 2017). Although the SO₂ broadening

data are derived from a single line experiment (Chandra & Chandra 1963), the parameters in the frequencies of interest are consistent with recent laboratory results by Bellotti & Steffes (2015). The broadening values for our SO₂ lines of interest are approximately $1.8\text{--}2.0\times$ air broadening (i.e. $\gamma_{\text{CO}_2} \simeq 0.17\text{--}0.19 \text{ cm}^{-1} \text{ atm}^{-1}$). For HDO, we multiply the HITRAN air foreign broadening parameters by 2.4, which is consistent with this frequency range (Sagawa et al. 2009).

To better visualize individual line signal and compare to the published data, we processed our flux spectra to normalize the continuum. Because we are processing noiseless model results, we mask spectral intervals for individual lines and linearly interpolate the continuum across the interval. The line:continuum (l:c) spectra were determined by dividing the original model spectrum by the continuum and subtracting one.

As an additional validation of our radiative transfer model and fit to the Greaves et al. (2020a) JCMT data, we applied our model to simulate the line shape and peak intensity of the 346.65 GHz late-2011 observation of Encrenaz et al. (2015), using their SO₂ profile of 10 ppb from 86–100 km, and obtained an excellent fit to the data (see Fig. 2).

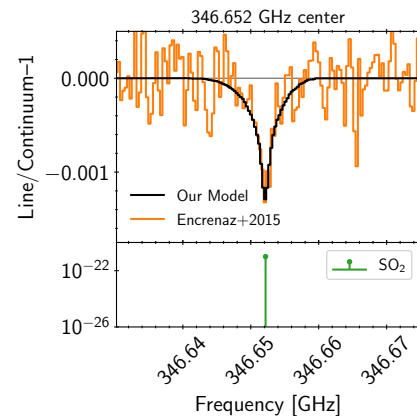


Figure 2. We demonstrate the validity of our model by fitting the 346.652 GHz SO₂ line observed by Encrenaz et al. (2015, Fig. 19) in 2011 using their best-fit profile of no SO₂ from 70–85 km and 10 ppb above 85 km, with all other modeling parameters specified as for our Case D (but also including CO from the De Bergh et al. (2006) compilation). SO₂ absorption line strength in the bottom panel is given in units of $\text{cm}^{-1}/(\text{molecule cm}^{-2})$. This comparison shows our model and associated parameters are consistent with previous sub-mm observations of SO₂.

3. RESULTS

To explore the spectral impacts of different abundances and vertical profiles for PH₃ and SO₂, we simulated spectra of Venus from 266 to 268 GHz. This spectral range includes the HDO, PH₃ and SO₂ line positions discussed in Greaves et al. (2020a), as well as OCS, which includes a

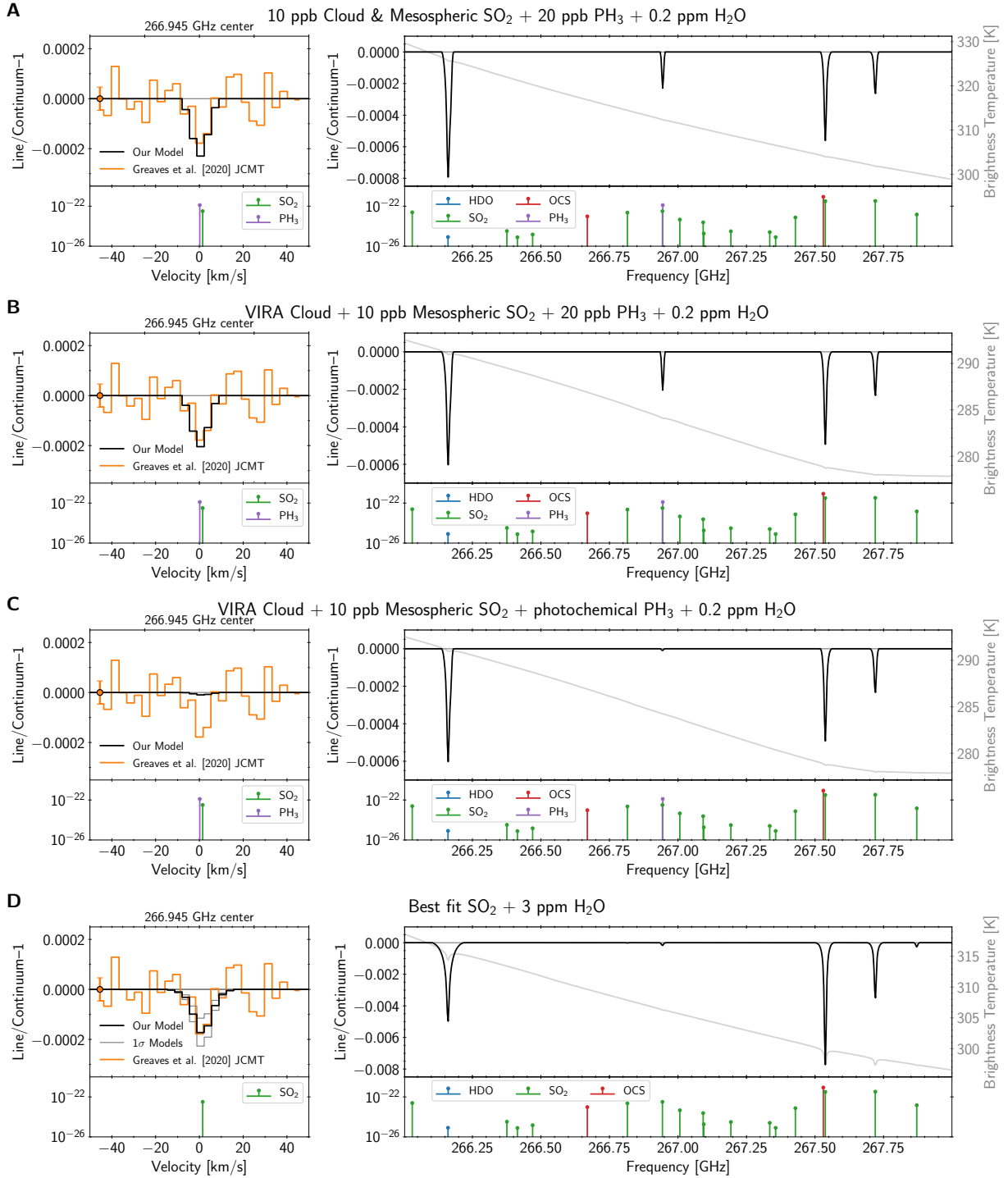


Figure 3. Venus spectral simulations for different PH_3 and SO_2 abundances and vertical profiles, including brightness temperature spectra (grey lines) to show the continuum source, and absorption line strengths (lower panels in each case) in units of $\text{cm}^{-1}/(\text{molecule cm}^{-2})$. For each case, the left hand panel shows the corresponding fit to the 266.94 GHz line, the right panel shows the 266–268 GHz spectrum, including the SO_2 reference line at 267.54 GHz. *Case A*: modified VIRA temperature and gas profiles with uniformly mixed 20 ppb PH_3 and 10 ppb SO_2 down through the cloud deck (c.f. Figure 1 Panel a). *Case B*: Case A but with the VIRA SO_2 profile in the cloud deck up to 70 km instead of evenly mixed at 10 ppb. *Case C*: VIRA and SO_2 profile as in Case B, but using the photochemically self-consistent profile for PH_3 from Greaves et al. (2020a) (ED Fig. 9). *Case D*: VIRA-2 temperature profile, no PH_3 , and using a vertically-resolved SO_2 profile derived from a suite of spacecraft and ground-based measurements, with a mesospheric profile that increases from 30 ppb at 78 km to 400 ± 150 ppb at 100 km (see Figure 1, panel b). Cases A and B demonstrate similar fits for PH_3 to the the 266.94 GHz line as in Greaves et al. (2020a), and show lack of sensitivity to the vertical distribution of SO_2 in the clouds. Case C demonstrates that the PH_3 profile generated assuming a source in the Venus clouds is inconsistent with the observed 266.94 GHz line. Case D shows that we can fit the detection feature with no PH_3 but with a typical Venus SO_2 abundance, although this produces SO_2 reference line features that are over 10 times stronger than the other cases.

transition at 267.530 GHz. We simulated spectra for cases with the abundances determined by Greaves et al. (2020a) and vertical profiles determined by previous measurements of the Venus atmosphere (Figure 1). Line-to-continuum (l:c) spectra generated at 0.0001 cm^{-1} (3 MHz) resolution are shown in Figure 3, along with the emission brightness temperature in grey. The brightness temperatures demonstrate the effective altitude of continuum emission, and are directly correlated with SO_2 abundance in the cloud deck between 54–57 km, depending on the case. Lower cloud SO_2 abundance (10 ppb evenly-mixed) yields higher continuum emission from deeper in the atmosphere.

3.1. Simulated Spectra

For our Case A spectral simulation (Figure 3A) we assumed updated VIRI-derived profile (our Figure 1, see von Zahn & Moroz 1985; De Bergh et al. 2006) for all constituents except SO_2 and PH_3 . Following Greaves et al. (2020a), we assumed an evenly mixed abundance of 20 ppb PH_3 and 10 ppb SO_2 above 52 km altitude (near the base of the Venus cloud deck; green and purple dotted lines in Figure 1a). We also assumed their foreign broadening parameter for PH_3 of $0.186 \text{ cm}^{-1} \text{ atm}^{-1}$. Our model produces a comparable fit to Greaves et al. (2020a) for the 266.94 GHz line (c.f. their Figure 1). Additionally, with the evenly-mixed 10 ppb of SO_2 , we also confirm that the 267.54 GHz SO_2 line is below the spectral-ripple-inferred maximum limit on the l:c ratio (-0.0006).

In our Case B simulation (Figure 3B), instead of assuming the low 10 ppb SO_2 down through the cloud deck, we used the VIRI-derived profile such that the SO_2 abundance increased with cloud depth (green dashed line in Figure 1b). At the 56 km level, the SO_2 abundance is now closer to 20 ppm. The increased SO_2 opacity raises the emission layer to cooler levels of the atmosphere, as shown in the the brightness temperature difference between Cases A and B. This produces a small change in the SO_2 continuum, which results in only marginal differences in the intensities of the 266.94 GHz PH_3 line and the 267.54 GHz SO_2 line, and the latter is still consistent with the maximum limit in sensitivity due to spectral ripple. Thus the observed line intensities are largely insensitive to SO_2 abundance within the clouds.

In our Case C simulation (Figure 3C), we again used 10 ppb SO_2 in the mesosphere, increasing through the cloud deck (green dashed line in Figure 1a). However, instead of PH_3 evenly mixed throughout the atmosphere (as in Cases A and B), we used the photochemical profile for PH_3 used to interpret the 266.94 GHz detection, as provided in Greaves et al. (2020a, their ED Figure 9), and Greaves et al. (2020a, reproduced as the purple dashed line in our Figure 1a). This distribution is derived from the assumption that PH_3 production is concentrated within the cloud deck with abundance

dropping rapidly in the upper cloud deck and mesosphere, and more slowly towards the surface. The small absorption line present here at 266.94 GHz is due to SO_2 —no PH_3 absorption is visible in this spectral simulation. This indicates that the line core observation is not sensitive to PH_3 in the cloud, and demonstrates that the assumed profile in the Greaves et al. (2020a) and Bains et al. (2020) photochemical simulations are inconsistent with the JCMT observations.

In our Case D simulation (Figure 3D), we removed PH_3 from our atmosphere and fit the JCMT detection feature at 266.94 GHz using SO_2 alone. As described in §2, we used parameters for HDO, SO_2 , and OCS foreign broadening by CO_2 . We guided the mesospheric data fit for SO_2 using Venus Express UV/IR occultation data from Belyaev et al. (2012). This profile is consistent with cloud-top SO_2 abundances measured by Encrenaz et al. (2019) within a month of the Greaves et al. (2020a) JCMT observations. Our best-fit SO_2 profiles, fitting the observed line (black) and $\pm 1\text{-}\sigma$ about the line (grey) are shown in Figure 1b (green curves), with SO_2 increasing from 30 ppb at 78 km to 400 ± 150 ppb at 100 km. These abundance profiles are well within the range of measurements compiled in Belyaev et al. (2012) and Vandaele et al. (2017). This simulation provides an excellent fit to the JCMT detection line without PH_3 , and predicts a pair of SO_2 reference lines that have l:c ratios a factor of ~ 10 higher than those seen in the previous simulations.

3.2. Spectral Line Sensitivity

To confirm the altitudinal sensitivity of the 266.94 GHz line for key PH_3 and SO_2 vertical profiles, we calculated radiance Jacobians, i.e. the increase in top-of-atmosphere radiance as a function of perturbations to the abundances for SO_2 and PH_3 at each layer of our model atmosphere (Figure 4). The outgoing radiance will be most sensitive to regions of the atmosphere that contribute most to the spectral feature. The Jacobians show that the observed line cores for both gases originate from atmospheric pressures only as deep as ~ 400 Pa, corresponding to altitudes of ≥ 80 km, in the mesosphere. This absorption feature cannot be generated at levels within the cloud deck, where the background continuum emission originates. It must be generated well above this layer, where the absorbing gas is cooler and therefore absorbs more efficiently than it emits. The narrow width of the absorption line also suggests that it was formed at pressures substantially less than those of the cloud top (70 km, ~ 3000 Pa).

3.3. ALMA Line Dilution

While the non-detection of prominent SO_2 spectral features in the ALMA wideband data could indicate a low abundance, as argued by Greaves et al. (2020a), the estimation of this abundance was done without correcting for line dilution as a result of the ALMA observing geometry (Greaves

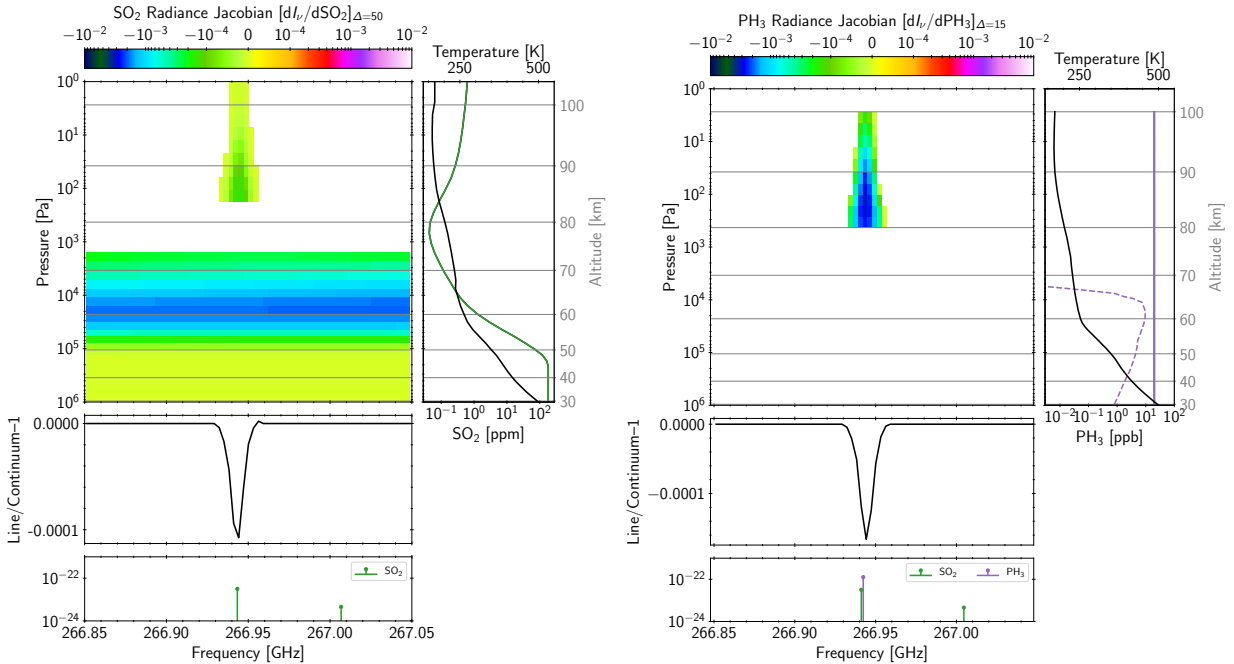


Figure 4. Radiance mixing ratio Jacobians (dl_v/dr_{mix}) as a function of layer pressure for the radiance streams at 21 degrees zenith angle, for the 266.94 GHz feature for SO_2 (left) or PH_3 (right). Absorption line strengths (lower panels in each case) are given in units of $\text{cm}^{-1}/(\text{molecule cm}^{-2})$. The continuum originates from SO_2 at $\sim 6 \times 10^4$ Pa (~ 54 km, within the cloud deck), while the line cores for either species do not originate in the clouds (48-70 km) but at over 400 Pa (over 80 km) in the mesosphere. In the right panels in both plots, the temperature structure is given as a black line, while the colored lines denote SO_2 (green) or PH_3 (purple) mixing ratios. On the right, the evenly-mixed 20 ppb PH_3 profile is shown with a solid line and the photochemical PH_3 profile is shown with a dashed line.

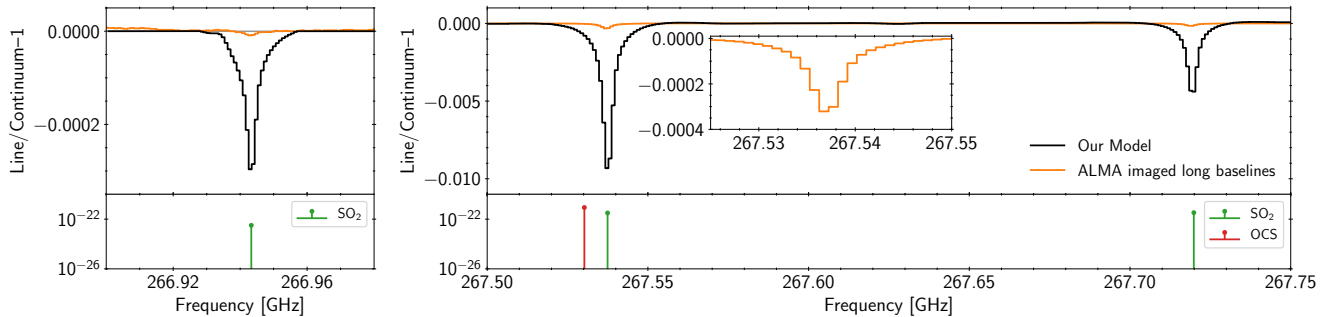


Figure 5. Modeled line dilution for the ALMA observations: disk-averaged line/continuum ratios for our nominal Case D atmosphere model containing SO_2 uniformly distributed over the Venus disk, at 0.00003 cm^{-1} (1 MHz) resolution (black lines), for the detection frequency (left panel) and reference lines frequencies (right panel). Absorption line strengths (lower panels) are given in units of $\text{cm}^{-1}/(\text{molecule cm}^{-2})$. The orange lines show the same spectral model as imaged using the ALMA antenna configuration of the Greaves et al. (2020a) observations. The inset shows the suppression of the 267.54 GHz reference line to an l:c of close to -0.0003 . The line intensity is significantly diluted, and is consistent with the non-detection of these SO_2 absorption lines in the wideband data.

et al. 2020a). Significant line dilution is likely, especially considering the global distribution of SO_2 in the Venus atmosphere, and the exclusion of the short baseline ALMA measurements. Greaves et al. (2020a) estimated line dilution (filtering losses) of 60–92% depending on position on the disk. To determine the disk-averaged line dilution for the SO_2 reference line search, we simulated observations of Venus using the ALMA configuration of Greaves et al. (2020a) by imposing an appropriate resolution spectrum (0.00003 cm^{-1} ,

1 MHz) of our Case D atmospheric model over a limb-darkened disk model. The Fourier Transform of this model was re-sampled to match the ALMA configuration and re-imaged using the imaging routines of Greaves et al. (2020a), as provided in their Supplementary Software 3. As shown in Figure 5, line dilutions on the order of 95% at the line core are observed for the full disk. We observe similar dilutions when the spectrum is only imposed on one hemisphere (~ 8 arcsecond extent at the time of observation). This line

dilution suggests that the SO_2 reference features produced by our best fit SO_2 distribution (Case D) would be heavily suppressed by line dilution in the ALMA data, which would cause them to mimic smaller features below the ripple detection limit of -0.0006 .

4. DISCUSSION

The claim that PH_3 has been detected in the Venus clouds is currently supported by observations of a single absorption line at a frequency that also coincides with absorption from SO_2 , a known and relatively common Venus gas, and based on an emission weighting function that peaks at 56 km (Greaves et al. 2020a). However, our radiative transfer analysis indicates that the line at 266.94 GHz does not measure absorption within the Venus clouds. Our explicit calculation of radiance Jacobians confirms the assessment that both 266.94 GHz PH_3 and SO_2 line core absorption would be produced well above the Venus cloud deck at altitudes exceeding 80 km. Arguments for a mesospheric origin for the 266.94 GHz line core, based on the observed narrow width of the line, are also provided in a recent commentary by Villanueva et al. (2020). This mesospheric contribution is inconsistent with a vertical abundance profile that concentrates PH_3 in the middle and upper clouds, as used by Greaves et al. (2020a) and Bains et al. (2020) to interpret their discovery. Our spectral simulation using this photochemical PH_3 profile also shows that it is not consistent with the strength of the observed 266.94 GHz line. However, the presence of PH_3 in the Venus clouds is not conclusively ruled out either, a point also made by Greaves et al. (2020b), because the Greaves et al. (2020a) observations are not sensitive to absorption at cloud deck altitudes, and so can neither exclude, nor confirm, the presence of PH_3 in the Venus clouds.

Given that we have shown that the observed 266.94 GHz line predominantly originates high in the mesosphere, attributing it to PH_3 is less chemically plausible than SO_2 . At these higher altitudes (>80 km) PH_3 would be destroyed rapidly, while SO_2 is photochemically regenerated (Sandor et al. 2010; Belyaev et al. 2012; Zhang et al. 2012). Between 82 km and 96 km (70–300 Pa, where the line core absorption originates, Fig. 4) PH_3 has a sub-second lifetime, due to the destruction by Cl and H radicals and UV photolysis (Bains et al. 2020). To balance this rapid destruction rate and maintain a mesospheric concentration of 20 ppb, an extremely large flux of PH_3 is required, potentially as large as 3.7×10^{15} molecules $\text{cm}^{-2} \text{s}^{-1}$. For comparison, this production rate is about ~ 100 times the flux of O_2 produced by Earth’s global photosynthetic biosphere (Field et al. 1998), the dominant metabolism on our planet. Greaves et al. (2020a), assuming the 266.94 GHz absorption was from PH_3 in the clouds, calculated a significantly smaller production rate of 10^7 molecules $\text{cm}^{-2} \text{s}^{-1}$, due to the lower destruction

rate within the clouds. However, the assumption of this in-cloud production rate results in a PH_3 mixing ratio that effectively falls to zero at >80 km altitude (Greaves et al. 2020a, Fig. 5b), which is inconsistent with our analysis that the observed line is sourced in the mesosphere. Although a recent reanalysis of the ALMA data by Greaves et al. (2020b) has greatly reduced the significance of the 266.94 GHz line detection, their assignment of 1 ppb of PH_3 in the mesosphere would still require a production rate significantly higher than the Earth’s photosynthetic biosphere, and the larger 20 ppb PH_3 value inferred from the JCMT data still stands.

These challenges to mesospheric production rate are not relevant if the observed 266.94 GHz line is instead attributed to SO_2 , which is known to increase in abundance with altitude in the mesosphere (Belyaev et al. 2012; Mills et al. 2018). A combination of infrared observations that probe the upper cloud and lower mesosphere, and UV occultation measurements that probe the upper mesosphere, has been used to map the vertical distribution of mesospheric SO_2 (Belyaev et al. 2012, 2017). This distribution drops from the cloud tops to a minimum just below 80 km, but increases substantially from 80–100 km to typically several hundred ppb (Belyaev et al. 2012; Vandaele et al. 2017).

Assuming that the Venus atmosphere does not contain PH_3 , we find that a realistic vertical profile for SO_2 fits the JCMT 266.94 GHz detection. Because the JCMT observations were single dish, any SO_2 contribution to the 266.94 GHz line would not have been suppressed, as was the case for the ALMA data, and so should be sensitive to the true mesospheric SO_2 abundance. We used a mesospheric SO_2 profile that is based on the profile observed in 2007–2008 by Belyaev et al. (2012), which is likely a good fit to similar higher values seen in 2016–2018, a time span that includes the Greaves et al. (2020a) JCMT observation. This profile is also consistent with cloud top values of 200–350 ppb observed in the mid-infrared within a month of the Greaves et al. (2020a) JCMT observations (Encrenaz et al. 2019). The Encrenaz et al. (2019) observations support the validity of our SO_2 vertical profile, and suggest that the Venus mesosphere was unlikely to be experiencing a period of anomalously low SO_2 abundance at the time of the JCMT observations. Using this vertical abundance profile and a CO_2 -broadened SO_2 line profile, we can fit the width and shape of the 266.94 GHz line using SO_2 alone, without needing an additional PH_3 component. The SO_2 is also a better fit to the line centroid than the PH_3 (cf. Fig. 3 A/B, D). This excellent fit counters the argument of Greaves et al. (2020b) that SO_2 alone would be too narrow to fit the observed line. Greaves et al. (2020b) also recently argued that the SO_2 abundance required to fit the JCMT 266.94 GHz line (evenly-mixed 150 ppb for their fit, and 100 ppb for Villanueva et al. 2020) is unrealistically large, given previous mm-wave observations,

which have returned lower values for mesospheric SO₂ (Santor et al. 2010; Encrenaz et al. 2015). However, mm-wave observations do not have as long, or as well sampled, a baseline as dedicated Venus spacecraft observations of the mesosphere (Belyaev et al. 2012, 2017; Vandaele et al. 2017), and mesospheric SO₂ abundance has been observed to vary by an order of magnitude on daily to yearly timescales, with values at 90–95 km altitude between 10 to 300 ppb. There is also evidence for longer-term secular changes in mesospheric and cloud-top SO₂ abundances, with maxima in 2007–2008 and 2016–2018, and a minimum in 2012–2014 (Belyaev et al. 2017; Encrenaz et al. 2019). We note that the model that we used to fit the JCMT 266.94 GHz line assuming a higher abundance of SO₂ also produced an accurate fit to the lower abundance observation of Encrenaz et al. (2015) (see our Fig. 2), which was observed near an SO₂ minimum.

We also find that strong ALMA line dilution allows the vertical abundance profile of SO₂ that fits the JCMT 266.94 GHz observations to still be consistent with the non-detection of the SO₂ ALMA reference lines—which are likely poor indicators of the impact of SO₂ on the JCMT observations. Spectral simulations using our Case D SO₂ vertical distribution predict SO₂ lines at 267.54 and 267.72 GHz with l:c ratios that are close to a factor of 10 larger than the nominal ALMA non-detection limit of -0.0006 given by Greaves et al. (2020a). This apparent contradiction can be reconciled by the lack of line-dilution in the JCMT observation of the 266.94 GHz line, as the single-dish integrates flux over all scales, while the telescope configuration and the removal of measurements from the ≤ 33 m ALMA baselines would have likely resulted in at least 90–95% line dilution (factor of 10–20 suppression) for spatially-uniform SO₂ gas. Therefore, taking the sensitivity of the two telescopes into account, our JCMT fit does not need to be adjusted, but our modeled SO₂ l:c ratios should be divided by at least ~ 20 , if the SO₂ is uniform across the disk, to approximate the ALMA detection for that set of baseline configurations. In doing so, our predicted SO₂ reference line values fall below the “10 ppb” (-0.0006) detection threshold (see Figure 5 inset). Consequently, the SO₂-only model with up to several hundred ppb of SO₂ in the mesosphere can fit the JCMT data, and still be consistent with the non-detection of SO₂ in the ALMA wide-band data. Moreover, this strong line dilution, with the corresponding loss of sensitivity to even high levels of SO₂, suggests that the ALMA wide-band SO₂ reference observations were likely poor indicators that SO₂ was low enough to be ruled out as a significant source of the JCMT 266.94 GHz line—thereby significantly weakening the argument that this line was instead due primarily to PH₃.

In addition to explaining the JCMT single-dish detection of the 266.94 GHz line, and the suppression of the SO₂ reference lines in the ALMA data, our SO₂-only hypothesis

would also predict that the 266.94 GHz ALMA line would be, like the SO₂ reference lines, strongly suppressed by line dilution and potentially non-detectable. While this was not the case in the original Greaves et al. (2020a) paper, this is now consistent with recent significant challenges to the detection confidence of the 266.94 GHz ALMA line. These include reanalyses of the Greaves et al. (2020a) narrowband ALMA discovery data by both Snellen et al. (2020) and Villanueva et al. (2020) who concluded that the feature attributed to PH₃ could not be detected with statistical significance. Our own further analysis of the Greaves et al. (2020a) ALMA data, including testing the robustness of the detection at 266.94 GHz, comes to a similar conclusion, and is presented in Akins et al. (accepted). Additionally, a recent reanalysis of high-resolution, S/N ~ 1000 Venus observations taken in 2015 was used to search for a PH₃ transition near 10.47 μm , but it was not detected, setting a stringent upper limit of 5 ppb above the Venus clouds (Encrenaz et al. 2020). Finally, the recent Greaves et al. (2020b) communication analyzing a reprocessing of the ALMA data suggests that the 266.94 GHz feature in the narrow-band whole-planet ALMA data is now significantly reduced in detection significance from the original discovery paper ($4.8\text{-}\sigma$ vs $13.3\text{-}\sigma$), with an l:c of -2×10^{-5} , consistent with 1 ppb of PH₃. However, this much-reduced 266.94 GHz feature would also be consistent with line-diluted SO₂, which in our model would have l:c of -1 to -2×10^{-5} at this frequency, for line dilution in the range 95–97%—which is likely well within the range of potential line dilution (Akins et al. accepted).

Although the SO₂ hypothesis self-consistently explains our current understanding of the detection and non-detections in the JCMT and ALMA data, additional analyses and observations will be needed to more definitively discriminate between PH₃ and SO₂ as the source of the 266.94 GHz JCMT line. Re-observing Venus at 266.94 GHz will likely still be needed to independently confirm the discovery observation, and detection of an additional PH₃ absorption feature would provide a much stronger case for its presence in the Venus atmosphere. Future observations to confirm the PH₃ $J = 1 \leftarrow 0$ line detection should incorporate single dish measurements, which would not suffer from line dilution, or observations including the Atacama Compact Array (which includes shorter baseline measurements than the primary ALMA array). Because the SO₂ abundance is critical to the PH₃ identification for the ALMA data, we recommend that future attempts to confirm the ALMA PH₃ observations should also obtain near-simultaneous SO₂ measurements. The narrowband correlator configuration can be tuned to 266.94 GHz and to the frequencies of two nearby, stronger SO₂ lines (near 267.54 and 267.72 GHz). To mitigate the spectral ripple features that compromised measurement of the line intensities (Greaves et al. 2020a), these observations should occur when the ap-

parent angular diameter of Venus is smaller and therefore less resolved by the ALMA antennas.

Ultimately, the claimed detection of PH₃ in the atmosphere of Venus has underscored the necessity of identifying and assessing the context of the environment within which we find potential biosignatures. The identification of the 266.94 GHz line as due to PH₃, and its plausibility as a potential biosignature, is inextricably intertwined with the physical and chemical environment of the Venus cloud and above-cloud atmosphere. This initial, controversial detection has highlighted just how much we still need to understand about our sister planet, and how important that knowledge is in interpreting this discovery. If the 266.94 GHz line is confirmed, and conclusively attributed to PH₃, its presence in the mesosphere would require additional observations to understand potential sources and sinks, and the attendant (and as yet unknown) phosphorous chemistry that enables its persistence at these high altitudes. Moreover, if PH₃ is being generated abiotically, especially at these high altitudes, this would have negative implications for the robustness of PH₃ and other reduced gases to serve as biosignatures in oxidizing terrestrial atmospheres. Regardless of the outcome, additional targeted observations will reveal processes on a terrestrial planet that informs our understanding of our own world, and potentially a large number of exoplanets that may share a similar evolutionary path and current environment.

5. CONCLUSIONS

We simulated millimeter-wavelength Venus spectra to explore the vertical distribution and detectability of PH₃ and SO₂ in the Venus atmosphere. We find that the observations of the 266.94 GHz absorption line are insensitive to the abundance of PH₃ and SO₂ within the cloud deck. Instead, the observed absorption at this wavelength originates from the mesosphere at altitudes above 80 km. At these altitudes, PH₃ would be rapidly destroyed, such that 20 ± 10 ppb of PH₃ would require a flux of PH₃ to the Venus mesosphere that is ~ 100 times higher than the global production rate of photosynthetically-generated O₂ on Earth. Because PH₃ and SO₂ both absorb within the width of the line detected at 266.94 GHz, we emphasize that the identification of this

absorption line as due to PH₃ in both the ALMA and JCMT data relies heavily on the apparent low abundance of SO₂ inferred from the non-detection of an SO₂ reference line at 267.54 GHz in the ALMA data. However, we show that SO₂ absorption is likely heavily suppressed in the ALMA data. Using SO₂ vertical profiles within the range of previous observations (from 30 ppb at 78 km to 400 ± 150 ppb at 100 km)—including SO₂ observations taken within a month of the JCMT data—our model can fit the depth and width of the 266.94 GHz feature without PH₃. We also show that ALMA line dilution suppresses the values for nominal Venus mesospheric SO₂ to below the corresponding detectability limit set by Greaves et al. (2020a). Given the mesospheric altitude range, short chemical lifetime of PH₃, and consistency with existing mesospheric SO₂ abundances observed within a month of the JCMT observations, we argue that SO₂ provides a more self-consistent explanation for the 266.94 GHz feature than PH₃. Single dish observations optimized for Venus and used to assess the PH₃ detection and SO₂ abundance in the Venus upper mesosphere should be prioritized to discriminate between PH₃ or SO₂ as the source of the 266.94 GHz line.

6. ACKNOWLEDGEMENTS

This work was performed by the Virtual Planetary Laboratory Team, a member of the NASA Nexus for Exoplanet System Science, and funded via NASA Astrobiology Program Grant No. 80NSSC18K0829. Part of this work was conducted at the Jet Propulsion Laboratory, California Institute of Technology, under contract with NASA. Government sponsorship acknowledged. This work made use of the advanced computational, storage, and networking infrastructure provided by the Hyak supercomputer system at the University of Washington. We thank Jacob Lustig-Yaeger, Kevin Zahnle, and the anonymous reviewers for helpful comments.

Software: LBLABC (Meadows & Crisp 1996), SMART (Meadows & Crisp 1996), CARTA (Comrie et al. 2020), CASA (McMullin et al. 2007), Matplotlib (Hunter 2007), Numpy (van der Walt et al. 2011), GNU Parallel (Tange 2011), WebPlotDigitizer (Rohatgi 2018).

REFERENCES

- Akins, A., Lincowski, A. P., Meadows, V. S., & Steffes, P. G. accepted, Complications in the ALMA Detection of Phosphine at Venus
- Arney, G., Meadows, V., Crisp, D., et al. 2014, *Journal of Geophysical Research: Planets*, 119, 1860, doi: [10.1002/2014JE004662](https://doi.org/10.1002/2014JE004662)
- Bains, W., Petkowski, J. J., Seager, S., et al. 2020, arXiv e-prints, arXiv:2009.06499. <https://arxiv.org/abs/2009.06499>
- Bellotti, A., & Steffes, P. G. 2015, *Icarus*, 254, 24, doi: [10.1016/j.icarus.2015.03.028](https://doi.org/10.1016/j.icarus.2015.03.028)
- Belyaev, D. A., Montmessin, F., Bertaux, J.-L., et al. 2012, *Icarus*, 217, 740, doi: [10.1016/j.icarus.2011.09.025](https://doi.org/10.1016/j.icarus.2011.09.025)
- Belyaev, D. A., Evdokimova, D. G., Montmessin, F., et al. 2017, *Icarus*, 294, 58, doi: [10.1016/j.icarus.2017.05.002](https://doi.org/10.1016/j.icarus.2017.05.002)
- Bezard, B., de Bergh, C., Fegley, B., et al. 1993, *Geophys. Res. Lett.*, 20, 1587, doi: [10.1029/93GL01338](https://doi.org/10.1029/93GL01338)

- Chandra, K., & Chandra, S. 1963, *JChPh*, 38, 1019, doi: [10.1063/1.1733747](https://doi.org/10.1063/1.1733747)
- Comrie, A., Wang, K.-S., Ford, P., et al. 2020, CARTA: The Cube Analysis and Rendering Tool for Astronomy, 1.3.0, Zenodo, doi: [10.5281/zenodo.3377984](https://doi.org/10.5281/zenodo.3377984)
- Cottini, V., Ignatiev, N. I., Piccioni, G., & Drossart, P. 2015, *Planet. Space Sci.*, 113, 219, doi: [10.1016/j.pss.2015.03.012](https://doi.org/10.1016/j.pss.2015.03.012)
- Crisp, D. 1986, *Icarus*, 67, 484, doi: [10.1016/0019-1035\(86\)90126-0](https://doi.org/10.1016/0019-1035(86)90126-0)
- . 1997, *Geophys. Res. Lett.*, 24, 571, doi: [10.1029/97GL50245](https://doi.org/10.1029/97GL50245)
- De Bergh, C., Moroz, V., Taylor, F., et al. 2006, *Planetary and space Science*, 54, 1389
- Encrenaz, T., Greathouse, T. K., Roe, H., et al. 2012, *A&A*, 543, A153, doi: [10.1051/0004-6361/201219419](https://doi.org/10.1051/0004-6361/201219419)
- Encrenaz, T., Moreno, R., Moullet, A., Lellouch, E., & Fouchet, T. 2015, *Planet. Space Sci.*, 113, 275, doi: [10.1016/j.pss.2015.01.011](https://doi.org/10.1016/j.pss.2015.01.011)
- Encrenaz, T., Greathouse, T. K., Marcq, E., et al. 2019, *A&A*, 623, A70, doi: [10.1051/0004-6361/201833511](https://doi.org/10.1051/0004-6361/201833511)
- . 2020, *A&A*, 643, L5, doi: [10.1051/0004-6361/202039559](https://doi.org/10.1051/0004-6361/202039559)
- Esposito, L. W., Copley, M., Eckert, R., et al. 1988, *J. Geophys. Res.*, 93, 5267, doi: [10.1029/JD093iD05p05267](https://doi.org/10.1029/JD093iD05p05267)
- Field, C. B., Behrenfeld, M. J., Randerson, J. T., & Falkowski, P. 1998, *Science*, 281, 237, doi: [10.1126/science.281.5374.237](https://doi.org/10.1126/science.281.5374.237)
- Gelman, B. G., Zolotukhin, V. G., Lamonov, N. I., et al. 1979, *Pisma v Astronomicheskii Zhurnal*, 5, 217
- Glindemann, D., Edwards, M., Liu, J.-a., & Kuschik, P. 2005, *Ecological Engineering*, 24, 457, doi: [10.1016/j.ecoleng.2005.01.002](https://doi.org/10.1016/j.ecoleng.2005.01.002)
- Gordon, I. E., Rothman, L. S., Hill, C., et al. 2017, *Journal of Quantitative Spectroscopy and Radiative Transfer*, 203, 3, doi: [10.1016/j.jqsrt.2017.06.038](https://doi.org/10.1016/j.jqsrt.2017.06.038)
- Greaves, J. S., Richards, A. M. S., Bains, W., et al. 2020a, *Nature Astronomy*, doi: [10.1038/s41550-020-1174-4](https://doi.org/10.1038/s41550-020-1174-4)
- . 2020b, arXiv e-prints, arXiv:2011.08176, <https://arxiv.org/abs/2011.08176>
- Gruszka, M., & Borysow, A. 1997, *Icarus*, 129, 172, doi: [10.1006/icar.1997.5773](https://doi.org/10.1006/icar.1997.5773)
- Huang, X., Schwenke, D. W., Freedman, R. S., & Lee, T. J. 2017, *JQSRT*, 203, 224, doi: [10.1016/j.jqsrt.2017.04.026](https://doi.org/10.1016/j.jqsrt.2017.04.026)
- Hunter, J. D. 2007, *Computing In Science & Engineering*, 9, 90, doi: [10.1109/MCSE.2007.55](https://doi.org/10.1109/MCSE.2007.55)
- Krasnopolsky, V. A. 2010, *Icarus*, 209, 314, doi: [10.1016/j.icarus.2010.05.008](https://doi.org/10.1016/j.icarus.2010.05.008)
- . 2012, *Icarus*, 218, 230, doi: [10.1016/j.icarus.2011.11.012](https://doi.org/10.1016/j.icarus.2011.11.012)
- . 2013, *Icarus*, 225, 570, doi: [10.1016/j.icarus.2013.04.026](https://doi.org/10.1016/j.icarus.2013.04.026)
- . 2020, Vega X-Ray Fluorescence Spectroscopy: Chemical Composition of Venus Clouds, <https://agu.confex.com/agu/fm20/webprogram/Paper784811.html>
- Krasnopolsky, V. A., Belyaev, D. A., Gordon, I. E., Li, G., & Rothman, L. S. 2013, *Icarus*, 224, 57, doi: [10.1016/j.icarus.2013.02.010](https://doi.org/10.1016/j.icarus.2013.02.010)
- Lincowski, A. P., Lustig-Yaeger, J., & Meadows, V. S. 2019, *AJ*, 158, 26, doi: [10.3847/1538-3881/ab2385](https://doi.org/10.3847/1538-3881/ab2385)
- Lincowski, A. P., Meadows, V. S., Crisp, D., et al. 2018, *ApJ*, 867, 76, doi: [10.3847/1538-4357/aae36a](https://doi.org/10.3847/1538-4357/aae36a)
- Marcq, E., Bézard, B., Drossart, P., et al. 2008, *Journal of Geophysical Research (Planets)*, 113, E00B07, doi: [10.1029/2008JE003074](https://doi.org/10.1029/2008JE003074)
- McMullin, J. P., Waters, B., Schiebel, D., Young, W., & Golap, K. 2007, in *Astronomical Society of the Pacific Conference Series*, Vol. 376, *Astronomical Data Analysis Software and Systems XVI*, ed. R. A. Shaw, F. Hill, & D. J. Bell, 127
- Meadows, V. S., & Crisp, D. 1996, *J. Geophys. Res.*, 101, 4595, doi: [10.1029/95JE03567](https://doi.org/10.1029/95JE03567)
- Mills, F., Jessup, K. L., Yung, Y., & Petross, J. 2018, in 42nd COSPAR Scientific Assembly, Vol. 42, C3.1–5–18
- Moroz, V. I., & Zasova, L. V. 1997, *Advances in Space Research*, 19, 1191, doi: [10.1016/S0273-1177\(97\)00270-6](https://doi.org/10.1016/S0273-1177(97)00270-6)
- Picciali, A., Moreno, R., Encrenaz, T., et al. 2017, *A&A*, 606, A53, doi: [10.1051/0004-6361/201730923](https://doi.org/10.1051/0004-6361/201730923)
- Robinson, T. D., & Crisp, D. 2018, *Journal of Quantitative Spectroscopy and Radiative Transfer*, 211, 78, doi: [10.1016/j.jqsrt.2018.03.002](https://doi.org/10.1016/j.jqsrt.2018.03.002)
- Roels, J., Huyghe, G., & Verstraete, W. 2005, *Science of The Total Environment*, 338, 253, doi: [10.1016/j.scitotenv.2004.07.016](https://doi.org/10.1016/j.scitotenv.2004.07.016)
- Roels, J., & Verstraete, W. 2001, *Bioresource Technology*, 79, 243, doi: [10.1016/S0960-8524\(01\)00032-3](https://doi.org/10.1016/S0960-8524(01)00032-3)
- Rohatgi, A. 2018, *WebPlotDigitizer*, Austin, Texas, USA, doi: [10.5281/zenodo.1137880](https://doi.org/10.5281/zenodo.1137880)
- Sagawa, H., Mendrok, J., Seta, T., et al. 2009, *JQSRT*, 110, 2027, doi: [10.1016/j.jqsrt.2009.05.003](https://doi.org/10.1016/j.jqsrt.2009.05.003)
- Sandor, B. J., Clancy, R. T., Moriarty-Schieven, G., & Mills, F. P. 2010, *Icarus*, 208, 49, doi: [10.1016/j.icarus.2010.02.013](https://doi.org/10.1016/j.icarus.2010.02.013)
- Seiff, A., Schofield, J. T., Kliore, A. J., et al. 1985, *Advances in Space Research*, 5, 3, doi: [10.1016/0273-1177\(85\)90197-8](https://doi.org/10.1016/0273-1177(85)90197-8)
- Snellen, I. A. G., Guzman-Ramirez, L., Hogerheijde, M. R., Hygate, A. P. S., & van der Tak, F. F. S. 2020, *A&A*, 644, L2, doi: [10.1051/0004-6361/202039717](https://doi.org/10.1051/0004-6361/202039717)
- Sousa-Silva, C., Seager, S., Ranjan, S., et al. 2020, *Astrobiology*, 20, 235, doi: [10.1089/ast.2018.1954](https://doi.org/10.1089/ast.2018.1954)
- Tange, O. 2011, *login: The USENIX Magazine*, 36, 42, <http://www.gnu.org/s/parallel>
- Thompson, M. A. 2020, *MNRAS*, doi: [10.1093/mnras/slaa187](https://doi.org/10.1093/mnras/slaa187)
- van der Walt, S., Colbert, S. C., & Varoquaux, G. 2011, *Computing in Science and Engineering*, 13, 22, doi: [10.1109/MCSE.2011.37](https://doi.org/10.1109/MCSE.2011.37)
- Vandaele, A. C., Korabiev, O., Belyaev, D., et al. 2017, *Icarus*, 295, 16, doi: [10.1016/j.icarus.2017.05.003](https://doi.org/10.1016/j.icarus.2017.05.003)

Villanueva, G., Cordiner, M., Irwin, P., et al. 2020, arXiv e-prints,
arXiv:2010.14305. <https://arxiv.org/abs/2010.14305>

von Zahn, U., & Moroz, V. I. 1985, *Advances in Space Research*,
5, 173, doi: [10.1016/0273-1177\(85\)90201-7](https://doi.org/10.1016/0273-1177(85)90201-7)

Wilzewski, J. S., Gordon, I. E., Kochanov, R. V., Hill, C., &
Rothman, L. S. 2016, *JQSRT*, 168, 193,
doi: [10.1016/j.jqsrt.2015.09.003](https://doi.org/10.1016/j.jqsrt.2015.09.003)

Zasova, L. V., Moroz, V. I., Esposito, L. W., & Na, C. Y. 1993,
Icarus, 105, 92, doi: [10.1006/icar.1993.1113](https://doi.org/10.1006/icar.1993.1113)

Zhang, X., Liang, M. C., Mills, F. P., Belyaev, D. A., & Yung, Y. L.
2012, *Icarus*, 217, 714, doi: [10.1016/j.icarus.2011.06.016](https://doi.org/10.1016/j.icarus.2011.06.016)

Zhu, R., Glindemann, D., Kong, D., et al. 2007, *Atmospheric
Environment*, 41, 1567, doi: [10.1016/j.atmosenv.2006.10.035](https://doi.org/10.1016/j.atmosenv.2006.10.035)